Microstructures

DOI: 10.1002/anie.200804194

How Rigid Rods Self-Assemble at Curved Surfaces**

Weizheng Zhou, Jian Cao, Weichang Liu, and Simeon Stoyanov**

Spherical or low-aspect-ratio particles have been used for producing superstable foams by tuning the particle wettability and interparticle interactions.[1–9] What is remarkable about these foams is that the stabilization against disproportionation arises from jamming in the adsorbed particle layer at a bubble surface,[10–13] rather than solidification or gelling of the continuous phase. Realizing the importance of particle shape, Alargova et al.[10,14,15] have developed a novel method for the preparation of flexible high-aspect-ratio microrods from epoxy resin; these rods were able to produce foams with excellent stability. Air bubbles stabilized by these rods have wool-ball or hairlike structures, in which rods are bended and entangled at the bubble surfaces.[10] When looking at these images an interesting question arises—what would happen if the rods become rigid and how would such rigid rods self-assemble at curved substrates, especially when the curvature and rod length are comparable?

To investigate this phenomenon, we used rigid $CaCO_3$ rodlike particles with a monomodal distribution in both diameter (0.5–1.0 μm) and length (10–30 μm; see Figure S1a in the Supporting Information). We chose the rod length to be comparable with the diameter of the smaller bubbles generated upon manual shaking, which allowed us to observe the self-assembly of these rigid rods on both large and small bubbles. Commercially available $CaCO_3$ rods are hydrophilic and have negligible surface affinity and foamability. We altered the particle hydrophobicity by modifying their surfaces with oleic acid[16] (see Figure S1b and S1c in the Supporting Information), which was expected to result in improved foaming properties.[3,10] However, dispersions of these modified $CaCO_3$ rods in distilled water produced hardly any foam, while quick aggregation and precipitation of the rods in the cylinder were observed. When ethanol (160 mM, 0.75 wt%) was added to these dispersions, they produced very fine foams with an excess of 50 vol% of air. These foams showed an excellent stability of longer than four months (see Figure S2a and S2b in the Supporting Information), which is comparable with that of other particle-stabilized foams.[4,6,10] The addition of a larger amount (10–90 vol%) of ethanol to particle dispersions has been previously used to change the solvent quality and improve particle wettability, foaming, and emulsification capacity.[3,17] However, in our case, the contact angle of modified rods against a solution of ethanol in water (2.0 wt%) was practically the same as that against distilled water, which indicated that the wettability of modified rods was hardly influenced by the presence of such a small amount of ethanol. We hypothesized that the role of ethanol is to switch off an effective sticky interaction between modified $CaCO_3$ rods, by partitioning into the fatty acid layer at the particle surface and improving its swelling in water. This in turn can lead to a weak short-range steric repulsion between two $CaCO_3$ rods, which counterbalances longer-range van der Waals attractions between weakly charged rods.[18] If this hypothesis is correct, other additives that can be partitioned between water and fatty acids should prevent the rods from sticking and trigger the foaming. Indeed the addition of less than 1 wt% of solvents such as tetrahydrofuran, acetone, or nonionic Polysorbate 20 or anionic sodium dodecyl sulfate surfactants at very low concentration (85 μM) gave the same result. This hypothesis was supported by an additional experiment in which the $CaCO_3$ rods were modified with γ-linolenic acid (GLA) instead of oleic acid. We expected that the higher degree of unsaturation of GLA would lead to better chain swelling in aqueous solution. Indeed, when shaken, dispersions of GLA-modified rods in distilled water showed foamability and stability comparable to oleic acid modified rods in presence of ethanol. We emphasize that the effect of alcohol or other specific additives or promoters is an important and novel method which made all subsequent structure formation possible.

The optical microscopy of bubbles stabilized by $CaCO_3$ rods (Figure 1) reveals that they are fully covered by the rods, are quasi-spherical with approximate diameters ranging from 10 μm to 200 μm, and show a distribution of large and small bubbles, which indicates a possible bimodal size distribution. The inset graph in Figure 1, obtained by manually measuring the bubble sizes in several images, confirms this observation; it shows clearly distinct peaks at 25 μm and 80 μm. Within the first 24 h, a few large bubbles relaxed their shape to become more spherical, but the bimodality was clearly observed. Upon prolonged storage over four months, no further changes in bubble shape and size were observed. One can expect that, at this initial stage, bubbles have many different shapes and sizes during the shaking process. The bimodal distribution mainly arises from the different fates of large and small

[*] W. Zhou,[+] Dr. J. Cao,[+] Dr. W. Liu
Unilever Research China, 3/F, Xin Mao Building
99 Tian Zhou Road, Shanghai, 200233 (P.R. China)
Fax: (+86) 21-5445-1625
E-mail: david.liu@unilever.com
Dr. S. Stoyanov
Unilever Foods and Health Research Institute
Olivier van Noortlaan 120, 3133 AT Vlaardingen (The Netherlands)
Fax: (+31) 10-460-6747
E-mail: simeon.stoyanov@unilever.com
[+] These authors contributed equally to this work.

[**] This work is partially supported by grant IS044065 from SENTER NOVEM, The Netherlands. We thank Dr. Vesselin Paunov (University of Hull, UK), Prof. Nikolai Denkov (University of Sofia, Bulgaria), Dr. Eddie Pelan, Dr. Theo Blijdenstein, Dr. Rob Groot, and Peter de Groot (Unilever Research, Vlaardingen, The Netherlands), and Dr. Gang Hu (Unilever Research, China) for useful discussions.
Supporting information for this article is available on the WWW under http://dx.doi.org/10.1002/anie.200804194.

InterScience DISCOVER SOMETHING GREAT
© 2009 Wiley-VCH Verlag GmbH & Co. KGaA, Weinheim

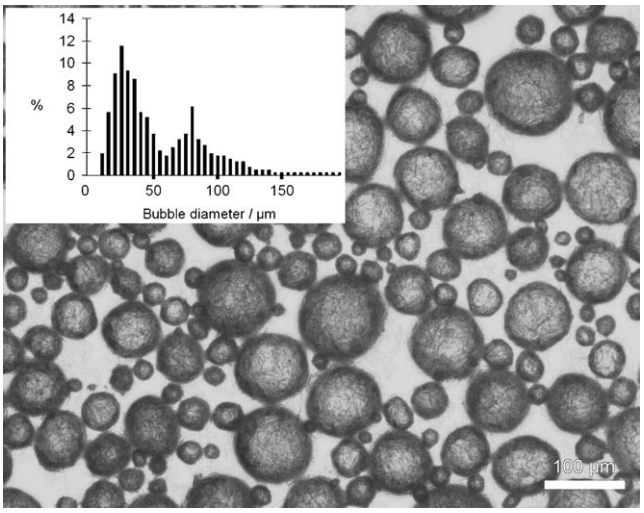

Figure 1. Optical micrographs of fresh bubbles stabilized by $CaCO_3$ rods modified with oleic acid. The inset shows the bubble size distribution, obtained by manual size measurement of approximately 400 bubbles from four different optical images, of the wet foam.[19]

bubbles during the shaking process, such as the attachment energy of the rods at interfaces, the deformation of bubbles, and coalescence and disproportionation, as well as the rod length and rigidity.

Figure 2 shows a series of scanning electron microscopy (SEM) images of single dry bubbles with increasing sizes. These images show that the air bubbles have preserved their spherical shape and have not collapsed during the drying process, which indicates that the surfaces of these bubbles are very rigid. For small bubbles with diameter of less than 30 μm, which is comparable with the average rod length, the rods overlap randomly with each other and assemble into a nestlike structure, where part of the rods stick out of the bubble surface into the continuous phase (Figure 2 a). It is apparent that the rigid rods are tangent to the bubble surface, which is different from the structure reported by Alargova et al.,[10] where flexible epoxy rods bend around the bubbles. When the bubble diameter is much larger than the rod length, the bubble curvature is low and rods can fully attach in a parallel orientation and form well-ordered 2D domains (Figure 2 d–f), producing a smectic-like crystal phase on the curved surface. In general, a bubble can have 10–50 domains, with each domain containing tens of rods. Transition structures with semiordered domains are shown in Figure 2 b and c.

Despite the difference in length scales and the nature of the materials, we find that the surface patterns observed on armored bubbles are remarkably similar to the domain structures formed on the river surface by large logs when transported from upriver to downstream (see Figure S2d in the Supporting Information). There is also a similarity with hierarchical structures of nanorods or nanowires[20–22] assembled by using the Langmuir–Blodgett technique, observed by Yang et al. and Whang et al., where surface order has been generated by manually compressing trough barriers, while in our case the order occurs spontaneously because of closed bubble topology, bubble shape relaxation, and disproportionation process in the initial stages after foam formation.[23,24]

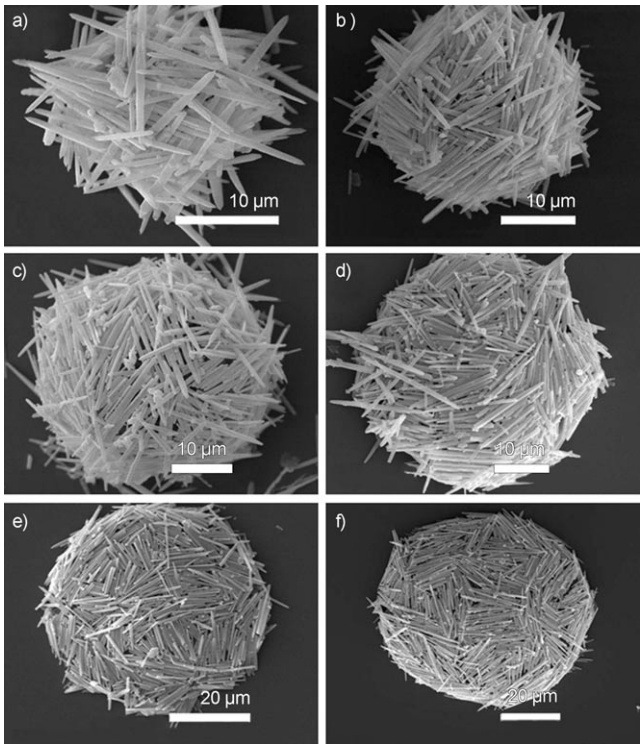

Figure 2. Microstructure evolution of bubbles stabilized by $CaCO_3$ rods: a) 20 μm bubble; nestlike microstructure with rods tangent to the bubble surface. b) and c) 30 μm and 40 μm bubbles; transition microstructure with overlapped rods and semiordered domains. d), e), and f) 50, 60, and 80 μm bubbles; armored microstructure with ordered domains constructed by highly oriented rods, especially for the 80 μm bubble (f).

Monte Carlo simulations of the phase behavior of two-dimensional hard-rod fluids also showed formation of 2D nematic phases,[25] depending on the surface coverage rod aspect ratio. However all these results relate to flat 2D geometries, while the image sequence in Figure 2 clearly demonstrates the important interplay between curvature and rod-length ratio and rod rigidity, which suggests that surface structures could be independently controlled and fine-tuned by these parameters as well.

Comparison of the SEM images of large dry bubbles (Figure 2 f) with the optical images of large wet bubbles floating on a water drop on a glass slide shows that very similar surface microstructures are present (see Figure S2c), which indicates that the drying process is of secondary importance for structure formation. Figure 3 shows the SEM image of dry broken bubbles, which were cut using a razor blade. It is clear that the inner surface of armored bubbles has a ordered domain structure that is similar to the outer surface, and the thickness of the bubble wall is about 1.0 μm (see insets in Figure 3), which is in the range of the rod diameter and indicates that the armored bubbles are stabilized by a monolayer of $CaCO_3$ rods. This is similar to the monolayer structure of bubbles stabilized by spherical polystyrene latex particles,[12] but different from the multilayer structure of bubbles stabilized by flexible epoxy resin rods,[10] in which the rods are flexible and can bend around the bubbles.

 © 2009 Wiley-VCH Verlag GmbH & Co. KGaA, Weinheim

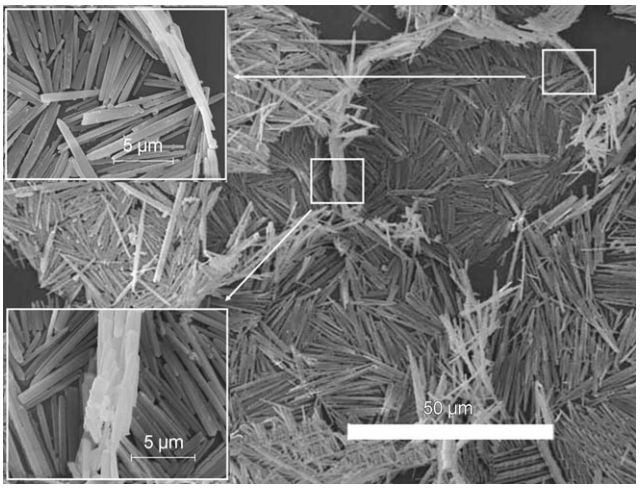

Figure 3. SEM images of dried and broken bubbles. A small amount of foam was placed on a drop of distilled water on a glass slide. After complete evaporation of the water, the dried bubbles were cut parallel to the glass slide by using a razor blade.

Furthermore, because of the superstability and rigidity of the bubbles, they can be assembled into 2D binary dry bubble crystals (Figure 4) following a similar approach to that used for the 2D assembly of colloidal particles[26,27] (see Figure S3 in the Supporting Information). A small amount of the foam produced in a shaking cylinder was taking using a pipette and placed on a drop of distilled water on a glass slide. Initially, all the bubbles floated on the water surface to form bubble rafts, in which small bubbles were located around large bubbles, without noticeable aggregation (Figure 1 and Figure S3a in the Supporting Information). During evaporation of the water, the layer became shallower and large bubbles were deposited on the glass substrate, forming a 2D crystal nucleus, while small bubbles still floated (see Figure S3b in the Supporting Information). Driven by the water evaporation flux, shrinking contact line, and capillary forces,[26] this nucleus of compacted bubbles grew into a 2D crystal-like structure.[27] Finally, the water layer became too shallow and small bubbles were deposited at the interstices between "ordered" large bubbles (Figure 4c and Figure S3c in the Supporting Information). This 2D binary structure of large and small bubbles is strikingly similar to the binary colloidal crystals constructed from a mixture of monodispersed spherical large and small solid particles.[28] Because of the polydispersity of the bubbles, the layers are far less ordered but bimodal effects are clearly observable (Figure 4b,c). By using other methods for bubble generation that allow generation of perfectly monodisperse bubbles, such as flow focusing or microfluidic devices, this direction could easily be further explored.

Single or binary colloidal crystals with 2D or 3D arrays where most of systems used solid and spherical particles have been widely studied.[28,29] The 2D bubble rafts (monolayers of ordered bubbles) on the surface of surfactant solutions[30] have been used to study 2D structures (e.g., of domains in metal alloys) or for studying foam rheology for decades. However, to the best of our knowledge, no examples in which bubbles were used to generate dry 2D structures by evaporation have been reported. The main reason is probably that bubbles stabilized by surfactants, proteins, or with spherical particles will collapse during the drying process, unless they are cross-linked or solidified beforehand.

When regarded from the bottom-up perspective, these 2D bubble crystals represent a remarkable self-assembly hierarchy, spanning over more than seven orders of length scale magnitudes: small changes in the degree of saturation of the fatty acid chain at the angstrom level have an effect on the self assembly of the fatty acid chains at the $CaCO_3$ rod surface at the nanometer level; this, combined with the rod topology, in turn influences the interaction between the rods and their self assembly at the bubble surface at the micrometer level and determining the bubble size distribution at millimeter level; this, in turn, determines the bubble ordering and self-assembly of solid substrates at the centimeter level. Similar to the lotus leaf, the 2D bubble crystals have inherent roughness on the nano- and micrometer levels, thus one can expect that, when replicated using the polydimethylsiloxane (PDMS) nanocasting approach of Sun et al.[31] or modified by deposition of thin layers and particles of transition metals partially fused by growing $CaCO_3$ crystals, one can obtain novel super water repellent surfaces. Similarly, if the bubbles in bulk 3D foams could be "glued" together and dried, the resulting product could be used as novel materials or material templates. This could provide a facile method for the development of novel light, porous materials, with improved isolation and mechanical properties, which could be used as

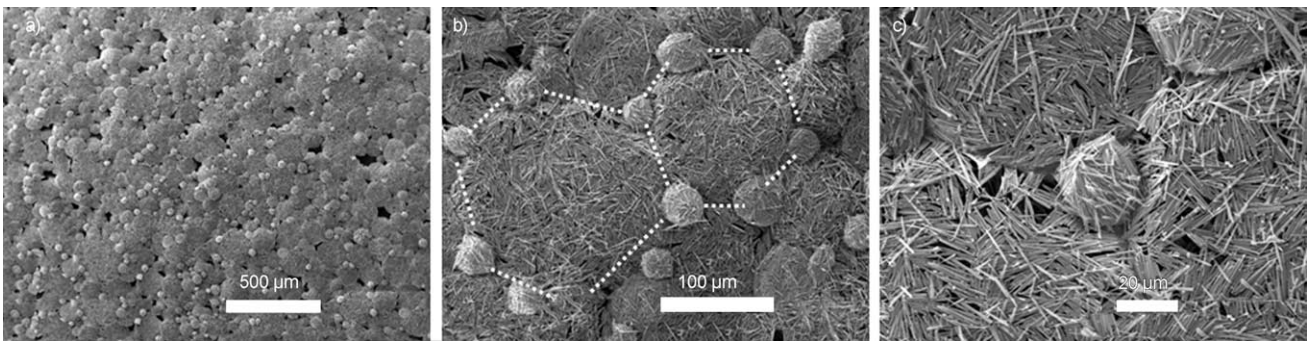

Figure 4. Binary 2D colloidal crystal constructed from rods stabilized by $CaCO_3$ bubbles. a) Overview SEM image of the hierarchical structure assembled on a glass slide. b) Magnified SEM image of hierarchical structure with "hexagonal" cells. c) Magnified SEM image of (b).

 © 2009 Wiley-VCH Verlag GmbH & Co. KGaA, Weinheim

substrates for catalysts, electrocatalysts, construction materials, separation membranes, or membranes for emulsification.

In summary, we have reported the production of superstable foams with a bimodal size distribution stabilized by modified $CaCO_3$ rods. The rigidity and high aspect ratio of $CaCO_3$ rods result in the first examples of unique bubble surface structures that evolve as a function of the curvature from nestlike to armorlike. The armorlike interface is composed of polydomains constructed from oriented rods, whose formation is analogous to the "logs on a river" process and determined by shear and confined surface. An interesting application could be in the area of colloidal liquid crystals assembled on curved interfaces. Because of their superstability and stiffness, bubbles stabilized by $CaCO_3$ rods are packed into 2D binary colloidal crystals, which show pronounced effects of bimodality. This novel 2D array of dried bubbles represents a hierarchy of self-assembled structures with dimensions from submicrometer to decimeter. These bubble arrays can be templated to produce novel materials with advanced hierarchical nano, micro, and macrostructures and specific properties.

The methods used to generate these structures are simple, scalable, and are based on sustainable materials. All the process and materials can be food grade, which allows the development of novel food systems, where the same material (fatty acid modified rods) could be used for structuring (delivering superstable aerated food products) and deliver health and nutrition in the same time when digested—$CaCO_3$ rods will dissolve at the low pH of the stomach and will release important nutrients and health actives like calcium and essential fatty acids.

Experimental Section

Methods: $CaCO_3$ rods with diameters of 0.5–1.0 μm and lengths in the region of 10–30 μm (Figure S1a in the Supporting Information) were supplied by Maruo Calcium Co., Ltd (Japan). Other chemicals were purchased from Sinopharm Chemical Reagent Co., Ltd (China). The modification of $CaCO_3$ rods was carried out by using a method similar to that reported previously.[16] After pretreatment at 500 °C for 3 h, $CaCO_3$ rods (10.0 g) were added to ethanol (100 mL) containing oleic acid (0.10 g). After stirring for 4 h at room temperature, the suspension was filtered and washed with ethanol (3 × 50 mL) to remove excess oleic acid. The filter cake was redispersed in ethanol (40 mL), and then distilled water (160 mL) was added into the dispersion with stirring. The dispersion was filtered and washed with distilled water (3 × 160 mL). Subsequently, the filter cake was added into distilled water to obtain an water dispersion (80.0 g), which was further lyophilized with a Labconco Freeze Dry System model 77530 (Labconco Corporation, USA) to obtain a free-flowing powder. The contact angle of the $CaCO_3$ rods changed from 41° to 81° after the modification (Figure S1b,c in the Supporting Information). Modified rods (0.5 g) were added to distilled water (10 g) in a 25 mL glass cylinder. Ethanol (0.075 g) was introduced into the mixture to tune the foaming properties. After sealing the cylinder with Parafilm, foam was produced at ambient temperature by shaking for 30 seconds by hand.

Instrumentation: Digital photographs of the foams were taken using a digital camera (DSC-F828, Sony, Japan). Optical photographs of the foams were obtained using an optical microscope (DM LB 2, Leica Microsystems Ltd, Germany). SEM images were obtained using a Philips XL 30 instrument. DSA 100 (Kruss, Germany) was used to measure the contact angle of the $CaCO_3$ rods after compressing the dry rods into a tablet.

Received: August 25, 2008
Published online: December 3, 2008

Keywords: fatty acids · foams · microstructures · self-assembly · surface chemistry

[1] B. P. Binks, *Curr. Opin. Colloid Interface Sci.* **2002**, *7*, 21–41.
[2] J. C. Wilson, PhD Thesis, University of Bristol, UK, **1980**.
[3] Y. Q. Sun, T. Gao, *Metall. Mater. Trans. A* **2002**, *33*, 3285–3292.
[4] B. P. Binks, T. S. Horozov, *Angew. Chem.* **2005**, *117*, 3788–3791; *Angew. Chem. Int. Ed.* **2005**, *44*, 3722–3725.
[5] A. Bala Subramaniam, M. Abkarian, L. Mahadevan, H. A. Stone, *Nature* **2005**, *438*, 930–930.
[6] U. T. Gonzenbach, A. R. Studart, E. Tervoort, L. J. Gauckler, *Angew. Chem.* **2006**, *118*, 3606–3610; *Angew. Chem. Int. Ed.* **2006**, *45*, 3526–3530.
[7] E. Dickinson, R. Ettelaie, T. Kostakis, B. S. Murray, *Langmuir* **2004**, *20*, 8517–8525.
[8] B. S. Murray, R. Ettelaie, *Curr. Opin. Colloid Interface Sci.* **2004**, *9*, 314–320.
[9] B. P. Binks, R. Murakami, *Nat. Mater.* **2006**, *5*, 865–869.
[10] R. G. Alargova, D. S. Warhadpande, V. N. Paunov, O. D. Velev, *Langmuir* **2004**, *20*, 10371–10374.
[11] A. L. Campbell, B. L. Holt, S. D. Stoyanov, V. N. Paunov, *J. Mater. Chem.* **2008**, *18*, 4074–4078
[12] S. Fujii, A. J. Ryan, S. P. Armes, *J. Am. Chem. Soc.* **2006**, *128*, 7882–7886.
[13] M. Abkarian, A. B. Subramaniam, S. H. Kim, R. J. Larsen, S. M. Yang, H. A. Stone, *Phys. Rev. Lett.* **2007**, *99*, 188301–188304.
[14] R. G. Alargova, V. N. Paunov, O. D. Velev, *Langmuir* **2006**, *22*, 765–774.
[15] R. G. Alargova, K. H. Bhatt, V. N. Paunov, O. D. Velev, *Adv. Mater.* **2004**, *16*, 1653–1657.
[16] M. A. Osman, U. W. Suter, *Chem. Mater.* **2002**, *14*, 4408–4415.
[17] B. M. Somosvari, N. Babcsan, P. Barczy, A. Berthold, *Colloids Surf. A* **2007**, *309*, 240–245.
[18] M. S. Romero-Cano, A. M. Puertas, F. J. de Las Nieves, *J. Chem. Phys.* **2000**, *112*, 8654–8659.
[19] U. T. Gonzenbach, A. R. Studart, E. Tervoort, L. J. Gauckler, *Langmuir* **2006**, *22*, 10983–10988.
[20] F. Kim, S. Kwan, J. Akana, P. Yang, *J. Am. Chem. Soc.* **2001**, *123*, 4360–4361.
[21] D. Whang, S. Jin, Y. Wu, C. M. Lieber, *Nano Lett.* **2003**, *3*, 1255–1259.
[22] P. Yang, *Nature* **2003**, *425*, 243–244.
[23] E. J. Stancik, M. J. O. Widenbrant, A. T. Laschitsch, J. Vermant, G. G. Fuller, *Langmuir* **2002**, *18*, 4372–4375.
[24] M. C. Friedenberg, G. G. Fuller, C. W. Frank, C. R. Robertson, *Langmuir* **1996**, *12*, 1594–1599.
[25] M. A. Bates, D. Frenkel, *J. Chem. Phys.* **2000**, *112*, 10034–10041.
[26] P. A. Kralchevsky, V. N. Paunov, I. B. Ivanov, K. Nagayama, *J. Colloid Interface Sci.* **1992**, *151*, 79–94.
[27] N. D. Denkov, O. D. Velev, P. A. Kralchevsky, I. B. Ivanov, H. Yoshimura, K. Nagayama, *Nature* **1993**, *361*, 26–26.
[28] K. P. Velikov, C. G. Christova, R. P. A. Dullens, A. van Blaaderen, *Science* **2002**, *296*, 106–109.
[29] A. Birner, R. B. Wehrspohn, U. M. Gosele, K. Busch, *Adv. Mater.* **2001**, *13*, 377–388.
[30] D. Weaire, S. Hutzler, *The Physics of Foams*, Oxford University Press, Oxford, **2000**.
[31] M. Sun, C. Luo, L. Xu, H. Ji, Q. Ouyang, D. Yu, Y. Chen, *Langmuir* **2005**, *21*, 8978–8981.

 © 2009 Wiley-VCH Verlag GmbH & Co. KGaA, Weinheim